

LINEAR COLLIDER DEVELOPMENT AT SLAC*

John Irwin

Stanford Linear Accelerator Center
Stanford, CA 94309

Abstract

Linear collider R&D at SLAC comprises work on the present Stanford Linear Collider (SLC) and work toward the next linear collider (NLC). Recent SLC developments are summarized. NLC studies are divided into hardware-based and theoretical. We report on the status of the NLC Test Accelerator (NLCTA) and the final focus test beam (FFTB), describe plans for ASSET, an installation to measure accelerator structure wakefields, and mention IR design developments. Finally we review recent NLC theoretical studies, ending with the author's view of next linear collider parameter sets.

1. SLC Status

The status of the SLC has been described elsewhere in these proceedings.^{1,2} This year's notable achievement is an increase of electron beam polarization at the IP from 23% to 63%. Also, luminosity is up from last year, and it is expected that this year's goal of 50,000 Zs on SLD (Stanford Linear Detector) tape will be achieved.

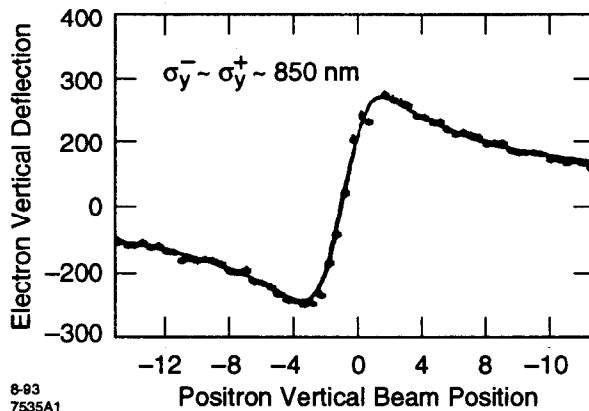


Figure 1. Typical beam-beam scans at the SLC interaction point with the current flat-beam operating conditions.

At the end of last year's run, during uncoupled damping rings tests for the FFTB collaboration, it was observed that small vertical emittances were well preserved down the linac and around the arc. When it was further realized that small vertical bumps in the arc could be used for spin rotation,³ eliminating the need for spin rotator solenoids which couple the betatron oscillation planes, it was decided to study flat beam operation at the start of this year's run. Operation in this mode has been successful and is now standard operating procedure.

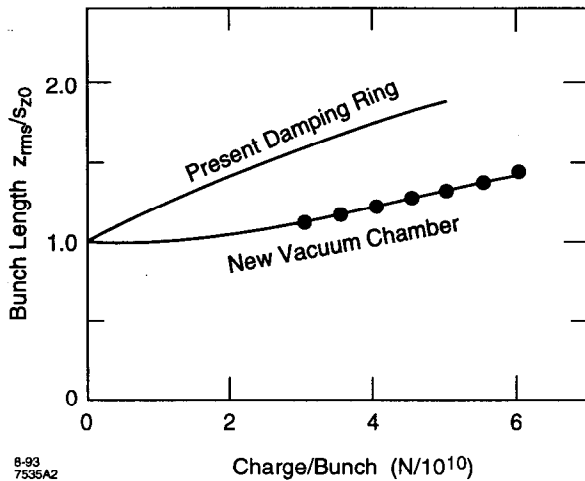
Figure 1 shows a recent beam-beam scan and corresponding beam sizes. This has opened the possibility of even higher luminosity through a final focus upgrade.

2. SLC Upgrade Plans

2.1. Damping ring upgrade

Impedance sources in the present damping rings have limited the bunch charge. As bunch charge is increased, an instability named the saw-tooth instability is encountered.⁴ The

* Work supported by Department of Energy contract DE-AC03-76SR00515.



8-93
7535A2

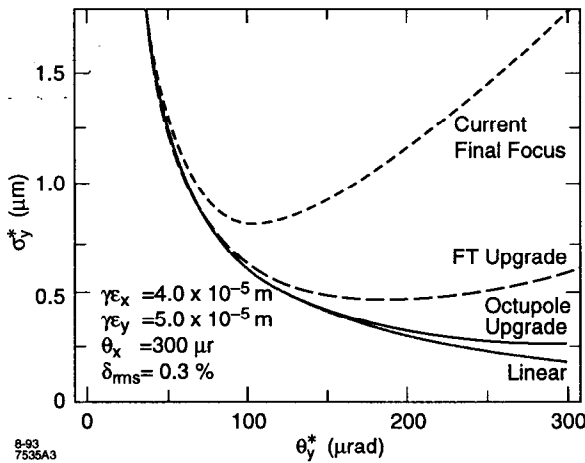
Figure 2. Bunch lengthening in the SLC damping ring with and without vacuum chamber upgrade.

onset of bunch lengthening from this instability is shown in Fig. 2. This is a doubly serious problem, since instabilities and variations in up-beam operating conditions make down-beam tuning and alignment very difficult, and in some cases impossible, as with wakefield compensation bumps.

Beginning in October, the vacuum system will be completely rebuilt. Table 1 compares the new ring impedance budget with the present ring. With this upgrade⁵ it is hoped that 3.5×10^{10} or more particles per bunch can be stably damped.

2.2. Final focus upgrade

If the IP divergent angle can be held constant as emittance is decreased by decreasing the vertical IP beta function, spot size will decrease linearly with the emittance rather than as the square root of emittance. This, however, implies larger beta functions in the SLC final focus systems, which in turn imply enhancement of sextupole and octupole aberrations. One of the octupole-like aberrations can be alleviated with the introduction of an additional quadrupole in the final telescope; the others require introduction of octupoles and sextupoles.⁶



8-93
7535A3

Figure 3. Spot size versus IP beta function with and without final focus upgrade.

The new quadrupole will be installed this fall, together with improved beam size diagnostics, expanded beta-match capabilities of the upper transformer, and improved power supply stability for the dipoles. During next year's run the octupoles will be installed together with small sextupoles to compensate final

doublet sextupole aberrations. The present $0.8 \mu\text{m}$ vertical spot dimension can theoretically be reduced to $0.5 \mu\text{m}$ without octupoles, and to $0.4 \mu\text{m}$ with octupoles (see Fig. 3).

Table 1. Impedance budget for the damping ring with and without vacuum chamber upgrade.

Present Vacuum Chamber, Single Element Inductance			Present Chamber, Contribution in Ring		New chamber inductance (ring contribution)	
Type	L[nH]	Factor	N	L[nH]	Remarks	L[nH] ring contr.
Bellows (no sleeves; not counted in inductance sum)	0.62	1.0	20	12.5	sleeved	<1
QD & QF masks	0.47	1.0	20	9.5	none	0
QF/D-bend transition	0.52	0.9	20	9.3	tapered	2.5
Ion pump slots	1.32	0.1	40	5.3		<1
Kicker bellows	2.03	1.0	2	4.1	sleeved	-
Flex joint	0.18	1.0	20	3.6	none	-
1" BPM transition	0.10	0.8	40	3.3	none	-
Other				2.4		2.4
			Total	37.5		6

3. Next Linear Collider Test Accelerator (NLCTA)

Figure 4 shows a plan view of the NLCTA facility currently under construction in end-station B at SLAC. It will contain an injector, an X-Band accelerator, and an output beam analysis spectrometer. The NLCTA will be a test-bed for, and an integration study of, the NLC X-band rf systems⁷ capable of addressing beam dynamics questions. The main X-Band acceleration section will contain three 50 MW klystrons equipped with independent modulators and SLED-II pulse compression systems capable of 4:1 power gains. Each klystron system will feed two 1.8 meter detuned acceleration structures. A second stage upgrade to six 100 MW klystrons is planned. This will increase the acceleration gradient from 50 MV/m to 100 MV/m. The first stage is scheduled for completion in early 1996.

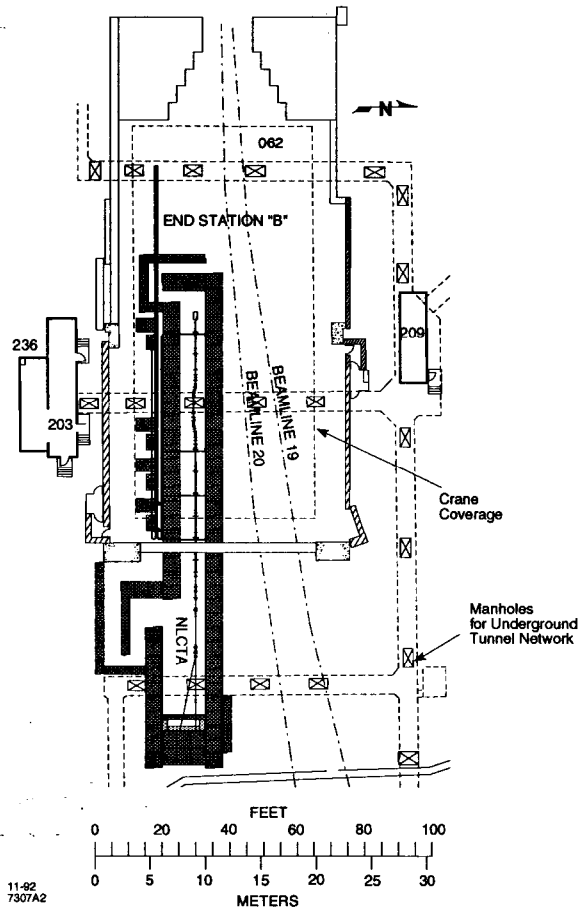


Figure 4. NLC Test Accelerator area plan view.

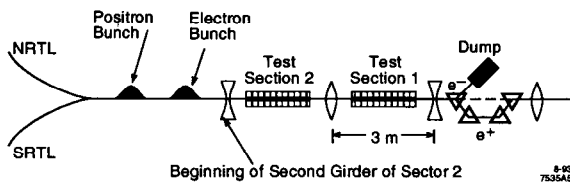


Figure 5. Schematic of the ASSET wakefield measuring elements.

observing changes in residual betatron motion of the second bunch as it travels down the SLAC linac. Leading bunch charge and time between bunches can be continuously varied.

5. Final Focus Test Beam (FFTB)

The final focus test beam is an international collaboration involving KEK, DESY, MPI (Munich), LAL (Orsay), INP (Novosibirsk), and SLAC.¹⁴ This facility will test next-generation final focus design principles as well as new advances in beamline systems. Such systems include stripline BPMs with 1 μm precision, magnet movers capable of

Design of the high efficiency modulators is complete and their construction will begin this summer.⁸ The first stage klystron goal of 50 MW 1 μs pulses has been achieved, and an ongoing program continues to improve klystron performance.⁹ The pulse compression system is now undergoing high power tests.¹⁰ The first prototype full-length acceleration sections are due this summer.¹¹ Accelerator structures, windows and rf components have been tested at SLAC in an area called the Accelerator Structure Test Area (ASTA). Breakdown studies have been done to surface field strengths of 500MV/m. Dark currents are acceptable up to 100 MV/m accelerating gradient. And rf windows capable of transmitting 100 MW klystron powers have been designed and tested, as well as components required for efficient rf transmission in overmoded wave guides.¹²

4. Accelerator Structure Setup (ASSET)

This facility, to be located in Sector 2 of the SLAC linac, is designed to measure wakefields of accelerator structures, which now can only be measured for short structures at the Argonne Accelerator Test Facility. See Fig. 5 for a schematic of ASSET.¹³ Required beamline changes will be put in place during the SLC down time this fall. By using an electron bunch from one damping ring followed by a positron bunch from the other damping ring, wakefields can be measured by

sub-micron vertical and horizontal steps, stretched-wire alignment systems capable of sub-micron measurements, improved wire beam size monitors, a new Compton, and a new ion beam size monitor for measurement of the 60 nm final spot size. All hardware is now in place, first beams have reached the dump, and radiation and beam containment system checks are complete. The first extensive commissioning of beamline hardware will take place in late August. Present operating emittances of the SLC meet requirements for the FFTB to achieve its design goals of a 60 nm high spot.

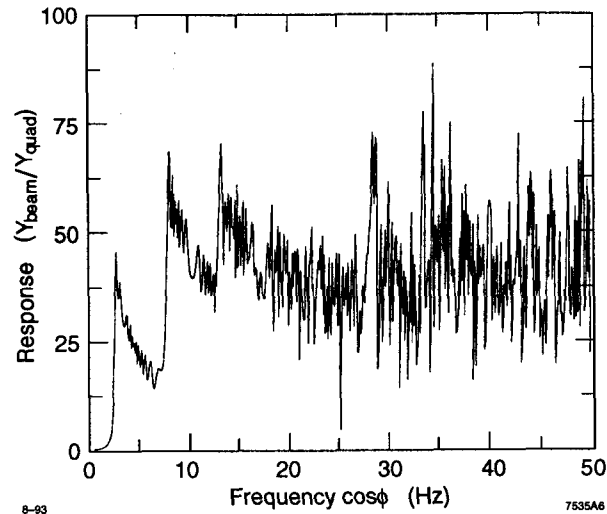
6. IR Design

IR design activity is reported elsewhere in these proceedings.^{15,16} It includes determination of quadrupole support design, masking requirements, geometric constraints, crossing angle requirements, luminosity monitors, background studies for all detector systems, detector sensitivities to low energy pairs and muons, beam size measurement devices, and bunch-to-bunch detector timing requirements. Of special importance is a new idea of G. Bowden for an inertial quadrupole in which a primary coil floats in the quadrupole field, and a secondary coil wrapped around the quadrupole is powered to create a small dipole field so that the flux in the primary coil remains unchanged. In other words, the quadrupole may move, but the field center will stay fixed, except at low frequencies where beam-based feedback can correct for motion.

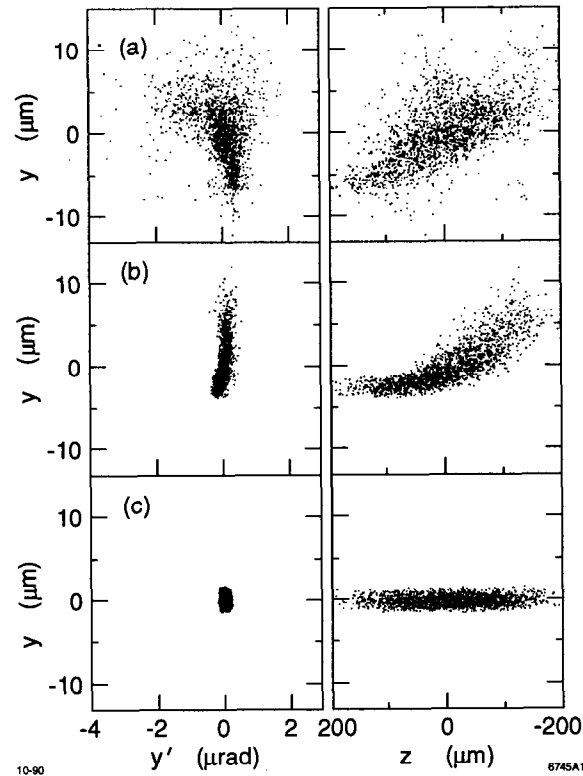
7. Theoretical Developments

7.1. Jitter Tolerances

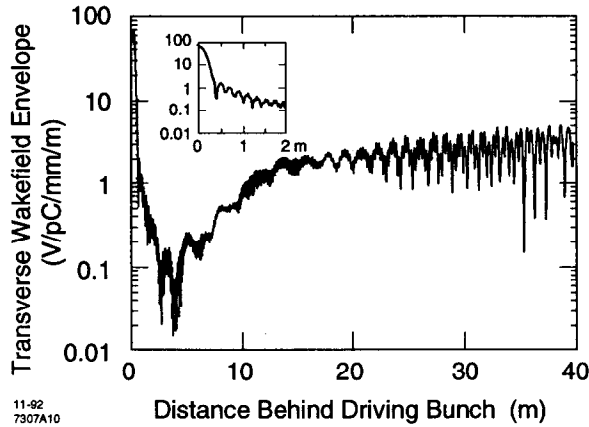
Jitter anywhere in the machine can result in beam jitter at the IP and a consequent loss in luminosity. In the SLC, several sources of vibration have been identified, including seismic and "cultural" ground motion. Feedback systems are essential and can reduce jitter at frequencies lower than 1/30 of the main 180 Hz repetition rate. Seismic motion above 6 Hz is small, but high frequency cultural noise sources must be isolated. Seismic motion in the 1 to 0.1 Hz range can be quite large, and would be a problem for feedback systems, except for the long-wavelength correlated nature of this motion. Figure 6 shows a plot of the beam motion response function as a function of ground motion wavelength.¹⁷ Note that, due to correlations, the response function is very small for frequencies below 2 Hz.



8-93
 Figure 6. NLC linac beam response function with correlated ground motion. 7535A6



10-90
 Figure 7. Emittance preservation in NLC linac with and without dispersion-free and wake-free steering. 6745A1



11-82
7307A10
Figure 8. Wakefield function for a detuned accelerating structure.

collimation and final focus systems perform properly. Theoretical work indicates that with properly ramped rf,¹⁸ the energy spread can be kept less than one part in 10^3 .

7.4. Detuned structures

Bunch trains with 90 bunches are contemplated. Residual ringing in accelerating structures can cause emittance growth. This can be overcome with damping, or alternatively by using a scheme which varies the cell dimension so as to change the frequency of the transverse modes in such a way that the transverse wakes cancel one another (see Fig. 8). Considerable progress has been achieved, and even with misaligned cavities little or no damping is required.¹⁹

7.5. Collimation system design

Reliable beam collimation is essential since one beam particle hitting the final doublet can blind the detector for a complete 90 bunch train. To ensure that the NLC is upgradeable, collimation and final focus systems have been designed to meet 1 TeV c.m. specifications. Figure 9 shows the beta functions for a complete conventional collimation system design that will collimate the beam to $5.5 \sigma_x$ and $35 \sigma_y$ and survive two bunch trains of a mis-steered beam. Limits on collimation depth arise from geometric and resistive-wall wakefields. Scrapers are assumed to be optimally tapered. The first collimation stage contains a 0.25-radiation-length plated carbon spoiler to protect the main absorber collimators. Each betatron phase must be collimated, and a second stage of collimation is required to clean up edge scattering from the first stage. Total collimation length for each linac of a 1 TeV c.m. collider is presently 1.5 km.²⁰

7.2. Emittance preservation in linac

Beam-based alignment techniques can be used to reduce linac BPM tolerance requirements. Figure 7 shows that with $70 \mu\text{m}$ BPM sensitivity, the beam emittance can be well-preserved if a beam-based alignment technique is used which varies the horizontally focusing and defocusing quadrupoles independently as families, realigning the beam so that it is stable under these strength variations.¹⁷

7.3. Multi-bunch energy compensation

The bunch-to-bunch energy spread within a train must be kept small so that

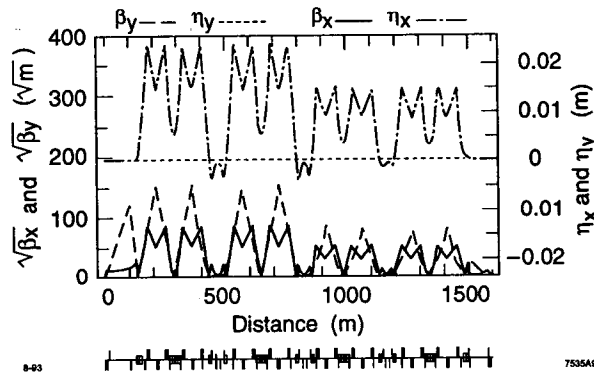


Figure 9. Lattice functions for a conventional NLC collimation system.

encourage attention to three features: location, location, location. Similarly, accelerator users desire: luminosity, luminosity, luminosity. The accelerator operating point will always be pushed to its luminosity limit. It follows, for example, that the limits of a particular design to align components should be determined and acknowledged as such and not presented as a loose tolerance feature.

Let us concentrate attention on the luminosity formula,

$$L = 1/4\pi N^2 f n_b / (\langle \sigma_x \rangle \langle \sigma_y \rangle).$$

The averages of transverse spot dimensions are included to indicate that, because of pinch effects, these quantities are not necessarily equal their linear design values. Typically $\langle \sigma_x \rangle$ is close to its linear value, while $\langle \sigma_y \rangle$ may be smaller. This luminosity formula may be rewritten as

$$L = 1/(8\pi \gamma mc^2) P_w \eta_w (N/\langle \sigma_x \rangle) (1/\langle \sigma_y \rangle),$$

where we have identified $2\gamma mc^2 N f n_b$ as the beam power in the two beams and replaced it by $P_w \eta_w$, the wall plug power times the efficiency of transforming wall plug power into beam power. All current designs have about the same value for P_w (200 MW).

The final three factors of this equation can be viewed as questions: is it efficient (η_w), is it clean ($N/\langle \sigma_x \rangle$), and can it be stabilized and aligned ($1/\langle \sigma_y \rangle$). In current parameter sets, the efficiency of TESLA is a factor of 4 larger than X-band, and $N/\langle \sigma_x \rangle$ is also a factor of 4 larger. The X-band claims to make up the luminosity in the precision it achieves with $\langle \sigma_y \rangle$. There is klystron research underway²³ aimed at achieving X-band wall plug-to-beam efficiency equal to the TESLA efficiency, $\eta_w = 20\%$.

Monte Carlo simulations indicate that muons produced in the collimator system will be sufficiently attenuated if a bend is placed after the collimator and if large torroids fill the tunnel cross-section at several locations.²¹ A 10–20 mr bend angle also provides the desired crossing angle at the IP. Two arcs, bending in opposite directions, each followed by its own final focus system, can allow for installation of two IPs.

7.6. Parameter Sets

Table 2 presents the current parameter list for the SLAC X-band NLC design. When buying a house, realtors

Table 2. Current NLC parameter set.

Parameter	500 GeV CM Energy	1 TeV CM Energy	Comments
E	250 GeV	500 GeV	Beam Energy
L ₀	6 x 10 ³³	1.2 x 10 ³⁴	Luminosity w/ Enhancement
L _H	9 x 10 ³³	2.0 x 10 ³⁴	
2 L _{Linac}	15 km	15 km	Total X-Band Linac Length
E _Z	50 MV/m	100 MV/m	Accelerating Gradient
f _{rf}	11.4 GHz	11.4 GHz	RF Frequency
N	0.65 x 10 ¹⁰	1.3 x 10 ¹⁰	Particles/Bunch
n _B	90	67	Number of Bunches
s _B	1.4 ns	1.4 ns	Bunch Spacing
f	180 Hz	120 Hz	Bunch Trains/sec
P _{beam}	4 MW	8 MW	Avg. Beam Power at IP
P _{wall}	140 MW	280 MW	Modulator Wall-Plug Power for Both Linacs
σ _x	300 nm	425 nm	variable
σ _y	3 nm	2 nm	γ ^{-1/2} scaling
σ _z	100 μ	100 μ	Bunch Length
δ _{RMS}	3 x 10 ⁻³	3 x 10 ⁻³	Energy Spread

For next generation machines, the upsilon parameter is small ($Y \leq 3$), from which it follows that²²

$$N/\langle\sigma_x\rangle = 1.8 \cdot 10^{16} n_\gamma \text{ and } \delta_B = 1.2 \cdot 10^{-11} (\gamma/\sigma_z) n_\gamma^2,$$

where n_γ is the number of photons produced by each electron during the beam-beam collision, and δ_B is the energy spread of initial beam particles due to photon production. It is because the number of background hadron events goes as n_γ^2 that we have identified $N/\langle\sigma_x\rangle$ with the question *is it clean*. Eliminating n_γ from the above relationships we have

$$N/\langle\sigma_x\rangle = 5.2 \cdot 10^{21} \delta_B^{1/2} (\sigma_z/\gamma)^{1/2}.$$

Since δ_B must be similar for all designs, we find that $N/\langle\sigma_x\rangle \sim \sigma_z^{1/2}$; one has the option of choosing a larger $N/\langle\sigma_x\rangle$ if one chooses a larger σ_z , though, as noted, this has the negative consequence of larger n_γ . Interestingly, a factor $\sigma_z^{-1/2}$ appears in $1/\langle\sigma_y\rangle$, since

$\sigma_y^2 = \epsilon_y \beta_y$ and β_y can be no shorter than σ_z ; hence no net luminosity advantage can be gained with the choice of large N ; one can only trade small $\langle \sigma_y \rangle$ problems for large N and n_γ problems.

Table 3 compares n_γ , N_{had} (the number of hadronic background events per bunch crossing), and δ_B for the latest available parameter sets for the X-band, S-band and TESLA designs. At 1 TeV c.m., energy spread and N_{had} parameters need improvement for the S-Band and TESLA designs.

Table 3. Comparison of X-Band, S-Band, and TESLA beam-beam quality indicators.

	n_γ	N_{had}	δ_B
0.5 TeV c.m.			
X-Band	0.9	.04	.03
S-Band	3	.3	.08
TESLA	4	.7	.04
1.0 TeV c.m.			
X-Band	1.1	.8	.07
S-Band	8	15	.5
TESLA	10	40	.5

We turn now to the question: will the next linear collider (NLC) be the last linear collider (LLC). In the large upsilon regime ($Y \geq 3$), appropriate to a 5 TeV machine,²²

$$N/\langle \sigma_x \rangle = 1.4 \cdot 10^{11} (\gamma/\sigma_z)^{1/2} n_\gamma^{3/2} \text{ and } \delta_B = 2/9 n_\gamma.$$

The second relationship implies that, for $\delta_B \leq 0.1$, we need $n_\gamma \leq 1/2$; hence

$$N/\langle \sigma_x \rangle \leq 0.5 \cdot 10^{11} (\gamma/\sigma_z)^{1/2}.$$

In this higher energy regime, the relationship with σ_z is reversed, and small σ_z is at a premium. To achieve a luminosity of $L = 25 \times 10^{34}$ at $\gamma = 5 \times 10^6$ (5 TeV in center-of-mass), assuming availability of $P_w = 400$ MW and $\eta_w = 25\%$, there is a solution with $\sigma_z = 10 \mu\text{m}$ and $\langle \sigma_y \rangle = 1/4$ nm. This occurs with $N/\langle \sigma_x \rangle = 3.5 \cdot 10^{16}$, not much different from present values. If hopes for inertial quadrupoles materialize, such values of $\langle \sigma_y \rangle$ may be possible. I will risk a prediction that the NLC will not be the LLC, and that these bunch lengths and precision requirements will be achieved with warm rf technology.

8. References

1. M. Breidenbach, SLC and SLD—Experimental Experience with a Linear Collider, these proceedings.
2. C. Prescott, Polarization Developments at the SLC, these proceedings.
3. T. Limberg, P. Emma, and R. Rossmanith, The North Arc of the SLC as a Spin Rotator, IEEE Particle Accelerator Conference Proceedings (May 93) and SLAC-PUB-6210.
4. P. Krejcik, et al., High Intensity Bunch Length Instability in the SLC Damping Ring, IEEE Particle Accelerator Conference Proceedings (May 93) and SLAC-PUB-6230.
5. K.L.F. Bane and C.-K. Ng, Calculation of Impedance for the Improved SLC Damping Rings, IEEE Particle Accelerator Conference Proceedings (May 93) and SLAC-PUB-6254.
6. N.J. Walker et al, Third-Order Corrections to the SLC Final Focus, IEEE Particle Accelerator Conference Proceedings (May 93) and SLAC-PUB-6207.
7. The Next Linear Collider Test Accelerator, J.M. Paterson, et al., IEEE Particle Accelerator Conference Proceedings (May 93) and SLAC-PUB-5928.
8. K. Harris, et al., 600kV Modulator Design for the SLAC Next Linear Collider Test Accelerator, IEEE Particle Accelerator Conference Proceedings (May 93) and SLAC-PUB-5851.
9. G. Caryotakis, et al., Development of Multimegawatt Klystrons for Linear Colliders, IEEE Particle Accelerator Conference Proceedings (May 93) and SLAC-PUB-6168.
10. C. Nantista, et al., High-Power RF Pulse Compression with SLED-II at SLAC, IEEE Particle Accelerator Conference Proceedings (May 93) and SLAC-PUB-6145.
11. R. H. Miller, et al., Accelerator Structure Work for NLC, IEEE Particle Accelerator Conference Proceedings (May 93) and SLAC-PUB-5865.
12. N.M. Kroll, et al., A High-Power SLED-II Pulse Compression System, IEEE Particle Accelerator Conference Proceedings (May 93) and SLAC-PUB-5782.
13. C. Adolphsen, et al., Measurement of Wakefields Generated in Accelerator Test Structures Using the SLC, XV International Conference on High Energy Accelerators, Hamburg, Germany (July '92) and SLAC-PUB-5941.
14. D. Burke, The Final Focus Test Beam Project, LC92 Proceedings (Aug. '92).
15. W. Ash, Summary of Experimentation Issues, these proceedings.
16. T. Markiewicz, Interaction Region Issues at the NLC, these proceedings.
17. T. O. Raubenheimer, The Preservation of Low Emittance Flat Beams, IEEE Particle Accelerator Conference Proceedings (May 93) and SLAC-PUB-6117.
18. K. A. Thompson and R. D. Ruth, Simulation and Compensation of Multibunch Energy Variation in the NLC, IEEE Particle Accelerator Conference Proceedings (May 93) and SLAC-PUB-6154.
19. K.L.F. Bane and R. L. Gluckstern, The Transverse Wakefield of a Detuned X-Band Accelerator Structure, submitted to Particle Accelerators and SLAC-PUB-5783; also K. A. Thompson, S. Adolphsen and K. L. F. Bane, Multibunch Beam Break-up in Detuned Structures, IEEE Particle Accelerator Conference Proceedings (May 93) and SLAC-PUB-6153.

20. J. Irwin, et al., Conventional Collimation and Linac Protection, IEEE Particle Accelerator Conference Proceedings (May 93) and SLAC-PUB-6198.
21. L.P. Keller, Calculation of Muon Background in a 0.5 TeV Linear Collider, contained in J. Irwin and D. Burke, Linear Collider IR and Final Focus Group Results, Research Directions for the Decade, Snowmass Proceedings (July 1990) and SLAC-PUB-5562.
22. K. Yokoya and P. Chen, Beam-beam Phenomena in Linear Colliders, US-CERN School on Particle Accelerators, Nov. '90, Hilton Head Island, S. Carolina, USA.
23. R. Palmer, The Amended Proposal for R & D on a Cluster Klystron, BNL-49420.